Subscriber access provided by University Libraries, University of Memphis

Article

Insights into the Complexity of Heterogeneous Liquid-phase Catalysis: Case Study on the Cyclization of Citronellal

Philipp Mueller, Patrick Wolf, and Ive Hermans

ACS Catal., **Just Accepted Manuscript** • DOI: 10.1021/acscatal.5b02493 • Publication Date (Web): 16 Mar 2016

Downloaded from http://pubs.acs.org on March 22, 2016

Just Accepted

"Just Accepted" manuscripts have been peer-reviewed and accepted for publication. They are posted online prior to technical editing, formatting for publication and author proofing. The American Chemical Society provides "Just Accepted" as a free service to the research community to expedite the dissemination of scientific material as soon as possible after acceptance. "Just Accepted" manuscripts appear in full in PDF format accompanied by an HTML abstract. "Just Accepted" manuscripts have been fully peer reviewed, but should not be considered the official version of record. They are accessible to all readers and citable by the Digital Object Identifier (DOI®). "Just Accepted" is an optional service offered to authors. Therefore, the "Just Accepted" Web site may not include all articles that will be published in the journal. After a manuscript is technically edited and formatted, it will be removed from the "Just Accepted" Web site and published as an ASAP article. Note that technical editing may introduce minor changes to the manuscript text and/or graphics which could affect content, and all legal disclaimers and ethical guidelines that apply to the journal pertain. ACS cannot be held responsible for errors or consequences arising from the use of information contained in these "Just Accepted" manuscripts.

ACS Catalysis is published by the American Chemical Society. 1155 Sixteenth Street N.W., Washington, DC 20036

Published by American Chemical Society. Copyright © American Chemical Society. However, no copyright claim is made to original U.S. Government works, or works produced by employees of any Commonwealth realm Crown government in the course of their duties.

Insights into the Complexity of Heterogeneous Liquid-phase Catalysis: Case Study on the Cyclization of Citronellal

Philipp Müller[a], Patrick Wolf[a,b], Ive Hermans[a,*]

[a] Department of Chemistry & Department of Chemical and Biological Engineering, University of Wisconsin – Madison, 1101 University Avenue, Madison, WI 53706 (USA)

[b] Department of Chemistry and Applied Biosciences, ETH Zurich, Vladimir Prelog Weg 2, 8093 Zurich (Switzerland)

ABSTRACT: Heterogeneously catalyzed liquid-phase reactions are highly complex chemical systems. As the local molecular composition close to the active site is often unknown, sophisticated spectroscopic tools are needed to gain insights on a molecular level. One solution to these challenges is the use of Modulation Excitation Spectroscopy with Attenuated Total Reflection Infrared Spectroscopy. We use this highly sensitive and selective technique to study the Lewis acid-catalyzed cyclization of citronellal over mesoporous Sn-SBA-15 and microporous Sn-Beta. We find that the reaction mechanism is generally similar with the two materials. However, the confined space at the active site within the zeolite stabilizes the coordination of citronellal to the Sn^{IV} site and prevents by-product formation, as well as the reverse reaction due to size-exclusion of the product isopulegol. The use of the Lewis base acetonitrile as solvent reduces the catalytic performance with Sn-SBA-15 drastically, while Sn-Beta remains highly active. Infrared spectra reveal a simultaneous coordination of citronellal and acetonitrile to the tin site in Sn-Beta, whereas in Sn-SBA-15 the better accessible Sn^{IV} site leads to much stronger and hence detrimental competitive adsorption. The results obtained in this study indicate that the substrate-catalyst-solvent combination needs to be optimized in order to maximize the performance of solid-liquid reactions.

KEYWORDS: modulation excitation, in situ infrared spectroscopy, confinement, solvent effect, stannosilicate, Sn-Beta

INTRODUCTION

In heterogeneous catalysis it is widely accepted that the catalytic performance does not only depend on the precise atomistic coordination of the active sites, but also on the embedment of these sites in the support material. For instance, catalysts with narrow pores of molecular dimension can trigger size-exclusion reactions,[1] or induce confinement effects that influence both the activity and selectivity.[2,3] Specifically for liquid-phase reactions, also the solvent (composition) can affect the overall performance of the catalytic system (*vide infra*). All these effects are often encountered in Lewis acid-catalyzed liquid-phase catalysis. Indeed, solid Lewis acids are widely used catalysts for various reactions, *e.g.* in biomass upgrading,[4] selective oxidations/hydrogenations[5,6] and the production of fine chemicals.[7] In particular, site-isolated Lewis acids incorporated in siliceous frameworks such as zeolites or (mesoporous) silicas have shown great potential, yet they are also notoriously complex.[8-12] Especially, Sn^{IV} incorporated in the BEA framework (Sn-Beta) obtained significant attention due to its exceptional activity and stability.[13] Two different types of active sites have been proposed, a four-fold framework-incorporated Sn^{IV} species (so-called closed site) and a partially hydrolyzed (so-called open) site, with tin three-fold bound to the zeolite framework.[14,15]

Not only does the nature of the active site play a role, but also its local molecular environment seems to influence the reactivity of Sn^{IV}-containing materials.[16] Testing Sn^{IV}-incorporated in microporous (*viz.*, Sn-Beta and Sn-MFI) and mesoporous catalysts (*viz.*, Sn-MCM-41 and Sn-SBA-15), Osmundsen *et al.* observed a distinct dependency of the activity for the conversion of biomass-derived substrates on the framework structure.[17]

As briefly mentioned above, a solvent can also affect the performance of a catalyst, *e.g.* by disturbing the substrate adsorption,[18] preferentially solubilizing certain molecules,[19] or altering the active site.[20] For instance, Boronat *et al.* studied solvent effects in the cyclization of citronellal to (-)-isopulegol, an important step in the artificial production of the flavoring agent (-)-menthol (see Scheme 1) over Sn-Beta.[21,22]

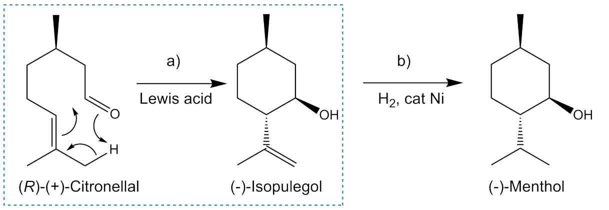

Scheme 1. Cyclization of (*R*)-(+)-citronellal to (-)-isopulegol, followed by the hydrogenation to (-)-menthol.

Adding the Lewis base acetonitrile to citronellal improves both activity and selectivity towards (-)-isopulegol. The authors hypothesize that both acetonitrile and citronellal adsorb to the Sn^{IV}-site, which results in enhanced stereoselectivity, due to a confined space around the catalytic center. Moreover, product desorption from the active site and diffusion inside the pores would be further facilitated by the presence of acetonitrile. Other solvents, such as longer chain nitriles and alcohols also affect the reaction. However, a general understanding of these effects is lacking, as a correlation between the catalytic performance and a single solvent characteristic, such as the dielectric constant or the molecular diameter, is not sufficient to capture the complexity of such catalytic systems.

A sensitive approach towards the understanding of heterogeneous liquid phase reactions, in particular on a molecular level, is vibrational spectroscopy.[23,24] For the cyclization of citronellal, an experimental FT-IR study has been performed, monitoring the disappearance of the characteristic vibrations of pre-adsorbed citronellal on Sn-Beta.[15] Two bands at 1729 cm^{-1} and 1715 cm^{-1} were observed and assigned to weakly and strongly adsorbed carbonyl groups, respectively. The presence of a C=C stretch vibration at 1645 cm^{-1} indicated the simultaneous formation of the isopulegol product. While valuable information can be provided by such an approach, many of the described effects are neglected, for instance due to the absence of solvent. Conclusive experimental studies under relevant conditions that address the mechanism on a molecular level are still missing.

In situ spectroscopic studies would in principle be able to provide this information. However, a poor signal-to-noise ratio as a consequence of low concentrations of active species is a frequently encountered problem that limits the applicability and interpretation of in situ spectroscopic studies. One highly sensitive and selective method to study reaction mechanisms at the solid-liquid interface is the application of a modulation excitation spectroscopy (MES) approach in combination with in situ attenuated total reflection infrared (MES-ATR-IR) and phase sensitive detection (PSD).[25] While the use of conditions that are close to actual reaction conditions are desirable for a spectroscopic study, they also impose significant complications. Indeed, in a solid-liquid reaction, multiple phenomena such as adsorption, (by-)product formation and desorption of various species occur simultaneously. It is hence difficult to distinguish between species that are actually involved in the surface reaction, *i.e.* active species, and those that just adsorb to the solid-liquid interface and do not react further, *i.e.* spectator species. PSD makes use of a mathematical treatment that is explained below, and transforms time-dependent spectra into phase-resolved spectra.[26] This transformation increases the signal-to-noise ratio, allows for differentiation between active and spectator species and simplifies the micro-kinetic analysis. This technique is hence ideal to shed light on the mechanisms involved in complex multiphase reactions.[27,28]

In the present work, we demonstrate the use of MES-ATR-IR in the case of the cyclization of citronellal, a model reaction of contemporary interest. Correlating macroscopic differences in the reactivity with a molecular understanding based on the information obtained from the solid-liquid interface allows us to draw conclusions on pore-size and solvent effects.

RESULTS

Materials & Batch reactivity

Three different Sn^{IV}-containing catalysts were synthesized following known procedures: an amorphous Sn-SiO$_2$,[29] a mesoporous Sn-SBA-15,[30,31] and a microporous Sn-Beta.[32-34] In addition, the siliceous analogues Si-Beta[35] and SBA-15[36] were prepared. Characterization of all synthesized materials is provided in the supporting information (Figures S1, S2 and Table S1).

The catalytic performance of these materials in the cyclization of citronellal was determined under batch reaction conditions with toluene and acetonitrile as solvent. Both solvents are widely used for carbonyl-ene reactions and strongly differ in polarity and size.[37] The diastereoselectivity was constant for all materials and solvents throughout the course of the reaction (see Figures S3 and S4). Overall higher activity was observed in toluene, where small amounts of products are already formed without a catalyst. In the presence of weakly Brønsted acidic SBA-15, both activity and selectivity increased. Significantly better catalytic performance was observed with the Lewis acidic stannosilicates, of which Sn-Beta yielded highest activity and diastereoselectivity, followed by Sn-SBA-15 and Sn-SiO$_2$. The achieved diastereoselectivity for Sn-Beta is slightly lower than reported values,[37] which could be explained by the post-synthetic preparation of the material. This leads to minor amounts of remaining silanol groups, possessing Brønsted acidity and slightly different active sites than in hydrothermal Sn-Beta.[38] An analysis of the Arrhenius plots (see Figures S6 and S7) indicates mass transfer to be influencing the reaction.

Table 1. Batch reactivity data for the cyclization of citronellal over different catalysts.[a]

Catalyst	Solvent	Conv. [%][b]	TOF [h^{-1}][c]	Sel. [%][d]	Sel.$_{dia}$ [%][e]
-	Toluene	4	-	50	67
SBA-15	Toluene	27	-	67	66
Sn-SBA-15	Toluene	89	115	92	64
Sn-SiO$_2$	Toluene	60	42	90	65
Si-Beta	Toluene	9	-	40	70
Sn-Beta	Toluene	66	185	89	70
-	Acetonitrile	-	-	-	-
SBA-15	Acetonitrile	-	-	-	-
Sn-SBA-15	Acetonitrile	15	12	50	65
Sn-SiO$_2$	Acetonitrile	7	6	0	0
Si-Beta	Acetonitrile	-	-	-	-
Sn-Beta	Acetonitrile	63	127	88	77

[a] Reaction conditions: 50 mg of catalyst, 5 mL of 0.5 M citronellal solution in solvent at 333 K, reaction time 4 hr.

[b] Conversion = (moles of citronellal initial - moles of citronellal after 4 hr)/moles of citronellal initial

[c] Turnover frequency (TOF) = moles of citronellal converted/moles of Sn after 1 hr

[d] Selectivity is defined as the moles of all produced isomers of isopulegol divided by the moles of converted citronellal

[e] Diastereoselectivity is defined as the moles of produced (-)-isopulgeol divided by the moles of all isomers of isopulegol produced.

With acetonitrile as the solvent, the blank reaction and the reaction with the pure silica materials, SBA-15 and Si-Beta, did not show any activity. Sn-Beta performed similarly in terms of selectivity compared to the reaction in toluene but was slightly less active. Conversely, Sn-SBA-15 is one order of magnitude less active when employed in acetonitrile and only reaches a selectivity of 50%, compared to 92% in toluene. One possible explanation for this is the competitive adsorption of acetonitrile and citronellal (both Lewis bases) to the Sn^{IV}-site. However, it is not readily clear why the activity only drops by 30% in the case of Sn-Beta, whereas it drops significantly more (about 90%) for Sn-SBA-15. These observations prompted us to perform a detailed in situ spectroscopic investigation. Due to the significantly lower activity of Sn-SiO_2, this material was not considered further.

Citronellal adsorption monitored with ATR-IR-MES

A suitable method to study adsorption/desorption dynamics, as well as reaction mechanisms at solid-liquid interfaces is ATR-IR spectroscopy combined with MES.[26,40,41] The latter follows an analogous principle as a lock-in amplifier by analyzing the response of a system to a periodic external stimulation, such as a change in temperature, radiation, pH, or as applied in the present work, reagent concentration. This approach is not only able to decrease the noise level to less than 10^{-5} absorbance units,[41] but also allows for the discrimination between active and spectator species. The application of PSD [eq. (1)] to the time-domain (TD) spectra transforms them into the phase-domain (PD), which further enhances the sensitivity and enables the extraction of (semi)-quantitative microkinetic data.

$$A_k \cos\left(\phi_k - \phi_k^{delay}\right) = \frac{2}{T}\int_0^T A(t)\sin(k\omega t + \phi_k)\,dt \qquad (1)$$

In equation (1), T is the length of one period, ω is the stimulation frequency, ϕ_k is the demodulation phase angle, $\phi_k{}^{delay}$ is the phase delay, k is the demodulation index (k=1 throughout this study), $A(t)$ is the active species response in the TD and A_k the response in the PD. The transformation to the PD leads to a dependence of the vibrational signals on the phase angle ϕ (adsorption from 0° to 180° desorption from 180° to 360°) instead of the time (60s adsorption; 60s desorption). In the following PD spectra, 36 phase-resolved spectra are shown with increments of 10° (corresponding to 3 seconds in the TD) which represent one whole period in the PD. In an ideal experiment, *i.e.* without diffusion limitation and immediate exchange of the cell volume (*i.e.* zero dead volume), the amplitude of the active species response, which corresponds to absorbance in the time-domain, would be 0 at 0° and 180°. A shift to larger phase angles can be attributed to hindered transport to the active site or, in the case of a reaction, to consecutive reaction steps. A detailed analysis of the spectra at various phase angles therefore provides valuable information on adsorption and reaction dynamics as will be demonstrated below.

To perform an ATR-IR MES experiment, the catalyst needs to be deposited as a thin film (ca. 15 µm) onto an ATR crystal. The penetration depth of an ATR experiment depends on the refractive indices of the sample and the crystal and is also wavelength dependent.[25] A rough estimation with the refractive index of SiO_2 (1.45) yields a penetration depth of 1-2 µm at 1000 cm^{-1}. Hence, mainly the pores within the catalyst particles are probed. The conditions for the spectroscopic experiments were chosen so that diffusion effects within the ATR cell are minimized and differences in phase delays can be attributed to diffusion within the catalyst as well as consecutive reaction steps (see Ref. 46 and experimental section for more details).

In order to investigate the catalytic cycle, the adsorption and reaction of citronellal was studied by switching between a solution of 20 mM citronellal in toluene and pure toluene. Figure 1a shows a projection of the TD of three averaged periods for the modulation over SBA-15 at 333 K. In the TD one major signal appears at 1727 cm^{-1}, which originates from the ν(C=O) vibration of liquid-phase citronellal (see Figure S8 for IR spectra of pure substances in toluene). At 1605 cm^{-1} the aromatic C-C vibration of the toluene solvent appears with a small negative absorbance band, indicating the displacement of toluene from the solid-liquid interface by citronellal. The transformation to PD allows for a more detailed analysis of the micro-kinetics and a more sensitive and selective detection of signals as only active species appear in the PD spectra. Furthermore, the clear assignment of an absolute phase delay to the corresponding maximum absorbance of a vibration in the TD makes a comparison between different experiments easier and allows for a semi-quantitative analysis. Figure 1c shows the PD spectra corresponding to the TD spectra from Figure 1a. The citronellal C=O peak appears with an absolute phase delay (*viz.* the maximum in PD) of 30°, which also corresponds to the minimum of the toluene band at the same angle. Furthermore, it is slightly skewed to lower wavenumbers, indicating only weak interactions with the solid catalyst. Complete citronellal desorption occurs at a phase angle of 220°, which can be seen by a maximum in the toluene peak and a minimum in the citronellal peak.

The incorporation of Sn^{IV} into the SBA-15 framework leads to different observations (Figure 1d). Next to the liquid-phase citronellal peak, a shoulder at 1712 cm^{-1} stemming from citronellal C=O groups interacting with the Sn^{IV} site appears at 50°, *i.e.* 20° (or 6 seconds) delayed compared to the liquid-phase peak. At 70°, a peak at 1643 cm^{-1}, assigned to the ν(C=C) vibration of the primary double bond in the product isopulegol, indicates that the catalytic reaction is taking place. Simultaneously, a red-shifted shoulder next to the liquid-phase peak appears, due to an interaction of isopulegol with either a Sn^{IV} site and/or the silica framework.[29,42]

For Si-Beta almost identical PD spectra were obtained as for SBA-15, but at larger phase angles (Figure 1e), indicating a longer time for citronellal to diffuse in the pores. When Sn^{IV} is incorporated into the Beta framework, the peak at 1712 cm^{-1} becomes significantly more intense than the liquid-phase citronellal peak at 1727 cm^{-1}. The more intense peak at 1643 cm^{-1} indicates increased productivity, in agreement with the batch experiments (see Table 1). Note that the C=O vibration of citronellal coordinated to Sn^{IV} appears at the exact same spectral position (1712 cm^{-1}) for both Sn^{IV}-containing materials, *i.e.* both catalysts perturb the C=O stretch vibration of citronellal to the same extent under reaction conditions. Even though the metal content in Sn-Beta is ca. three times lower than in Sn-SBA-15, the absolute coverage of citronellal coordinated to Sn^{IV} is clearly much higher in case of the zeolite. This observation suggests confinement effects as a likely reason for the increased productivity, rather than the stronger Lewis acidity of Sn-Beta (Ref. 16 and Figure. S10 for liquid-phase d_3-acetonitrile adsorption). The confined space inside the zeolite pore of molecular dimension (6.7 Å[43]) leads to more negative adsorption enthalpies due to van der Waals interactions[44] which might additionally stabilize the coordination of citronellal, resulting in increased coverage of the tin site.

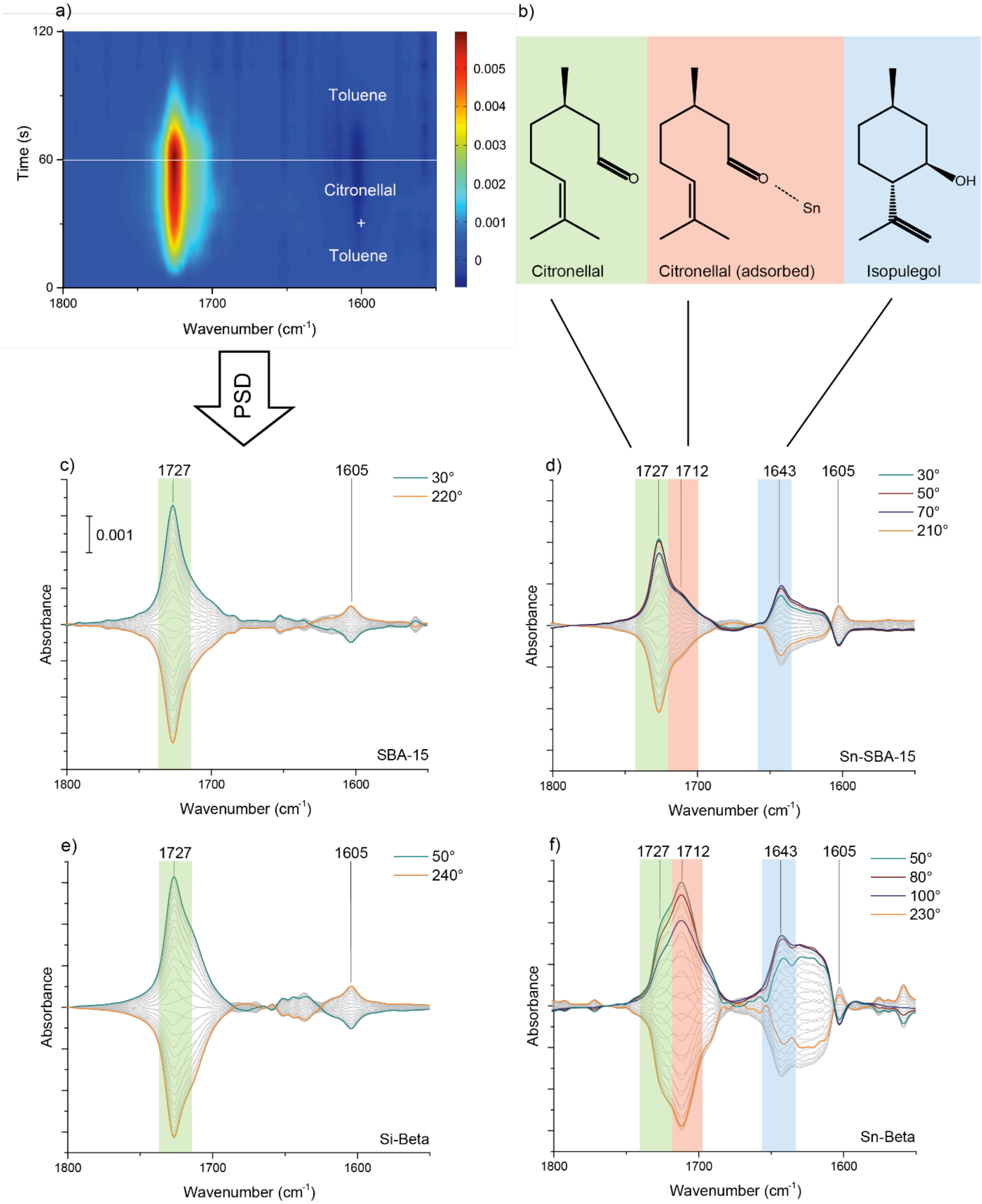

Figure 1. a) Time-domain spectra for the modulation of 20 mM citronellal in toluene at 333 K for SBA-15, b) Schematic representation of the most important molecular structures and their assignment, Phase-domain transformed spectra for c) SBA-15, d) Sn-SBA-15, e) Si-Beta and f) Sn-Beta.

Interestingly, the red-shifted product shoulder (ca. 1625 cm^{-1}), *i.e.* adsorbed isopulegol, is also more intense compared to Sn-SBA-15 and reaches a maximum at 80°, while the liquid-phase product peak reaches a maximum at 100°. This implies that the shoulder most likely originates from an isopulegol species inside the zeolite pore that might relax to a different conformation once it leaves the pore. Also the ν(OH) vibration of isopulegol appears as a broad signal centered at 3250 cm^{-1}, corroborating an interaction of isopulegol with the zeolite (Figure S25).

Under vacuum conditions, isolated Si-OH and Sn-OH bands show a signal at 3740 and 3664 cm^{-1} respectively (see Figure S9 and Ref. 3). Surprisingly, no significant change in either of these bands could be observed for both of the Sn^{IV}-containing catalysts upon the adsorption of citronellal from the liquid phase (Figures S14, S15, S24, S25). However, it is likely that the presence of a solvent shifts these signals to lower wavenumbers, broadens them and weakens their intensity.[45] The adsorption of citronellal on Sn-Beta leads to two negative bands, one at 3600 cm^{-1} and a smaller one at 3700 cm^{-1}, both bands are present in the low-defect Si-Beta as well but with lower intensity (Figures S17 and S18). We therefore assign the band at 3700 cm^{-1} to isolated Si-OH groups interacting with citronellal in Beta zeolites. Dealuminated Beta shows a distinct negative band at 3600 cm^{-1} at the same phase delay as the appearance of citronellal, which we therefore assign to an interaction of citronellal with silanol groups (Figures S19-S22). For an interaction of citronellal with a Sn-OH group, we would expect a signal at lower wavenumbers than the Si-OH peaks. This was however not observed. Hence, the present study does not confirm the direct participation of a Sn-OH group in the reaction mechanism for both Sn-Beta and Sn-SBA-15. Nevertheless, as many different species (isopulegol, Si-OH, Sn-OH, water impurities) possibly show a signal in this spectral region, and the concentration of Sn-OH species is supposed to be rather small, the absence of evidence cannot be interpreted as the evidence for absence. Testing another Beta sample with a ten times higher tin loading resulted in similar spectra and also no indication of a distortion of Sn-OH vibrations when adsorbing citronellal (see Figure S26). Yet, the above findings exemplify the consecutive steps needed for this reaction to occur: (1) citronellal coordinates to the Sn^{IV} site, (2) citronellal is converted to isopulegol inside the pores of Sn-Beta, (3) isopulegol interacts with either the Sn^{IV} site and/or the pore walls until (4) isopulegol diffuses out of the pore (*vide infra*). Additionally, the overall larger phase delays found for Sn-Beta compared to Sn-SBA-15 suggest diffusion limitations caused by the smaller pores in Sn-Beta.[46] As citronellal has a small kinetic diameter and is flexible (*viz.* it can freely rotate around its C-C bonds), it can diffuse more easily inside the zeolite pore channels and find its way to a tin site. The cyclization leads to a more rigid product with a larger kinetic diameter, inducing diffusion limitations inside the micropores. However, as the Sn^{IV} sites in Sn-Beta are embedded in a confined space stabilizing the coordination of citronellal, it still outperforms Sn-SBA-15.

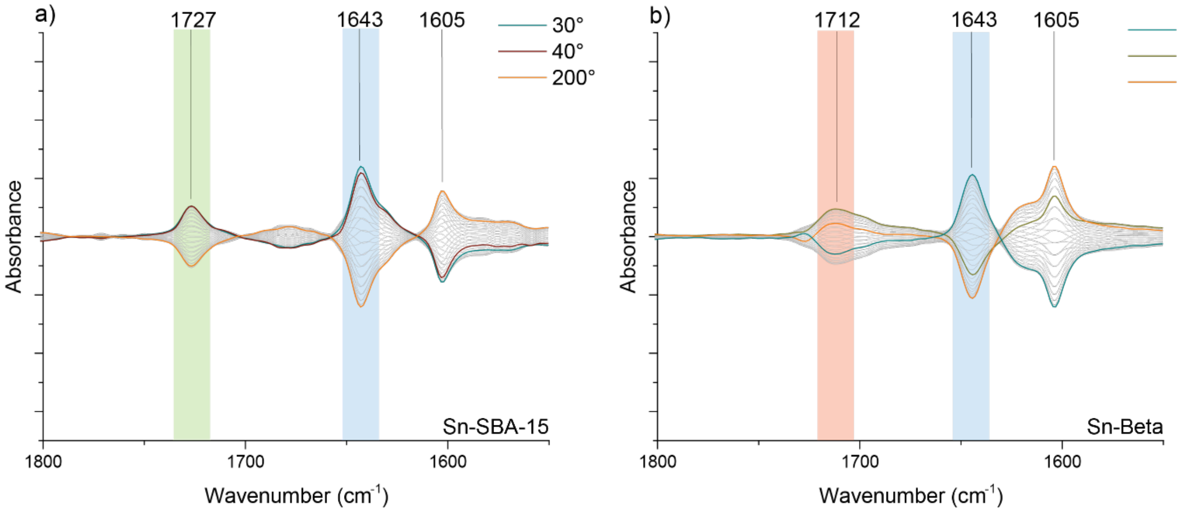

Figure 2. Phase-domain spectra of modulation experiments with 20 mM (-)-isopulegol in a solution of 20 mM of citronellal in toluene at 333 K for Sn-SBA-15 a) and Sn-Beta b).

Competitive adsorption of (-)-isopulegol and citronellal

In order to get insights into the competitive adsorption behavior of substrate and product, the concentration of (-)-isopulegol was modulated in presence of a constant citronellal concentration. In the case of SBA-15 and Si-Beta, a relatively sharp ν(C=C) vibration is visible at 1643 cm^{-1}, corresponding to liquid (-)-isopulegol (Figures S27-S30). For Sn-SBA-15 (Figure 2a), the spectra are significantly different. Other than expected, the liquid-phase citronellal peak (1727 cm^{-1}) appears. The absolute phase delay for this peak is 40°, which is 10° delayed from the C=C vibration of (-)-isopulegol, indicating a production of citronellal from (-)-isopulegol, *i.e.* the reverse reaction. However, compared to the reaction from citronellal a considerably smaller red-shifted shoulder next to the liquid-phase peak appears. In a further batch experiment (-)-isopulegol was used as substrate over Sn-SBA-15 and only little conversion was observed (see Figure S5), suggesting that this is only a minor effect on a macroscopic scale. When (-)-isopulegol is adsorbed on Sn-Beta (Figure 2b), its C=C stretch vibration appears at 1643 cm^{-1} and no red-shifted shoulder can be observed. In addition, a small and broad feature at 1712 cm^{-1} is visible with an absolute phase delay of 200°. This strongly suggests the adsorption of isopulegol to the few accessible external or pore mouth Lewis acid sites which leads to a distortion of the citronellal signal. In the TD spectra (Figure S31), the change in intensity is hardly visible, which further confirms that this is only a minor effect and demonstrates the increased sensitivity when applying PSD. The presented data demonstrate that (-)-isopulegol does not enter the zeolite pore and thus can only compete for the active site if it is formed inside the pores. Consequently the reverse reaction is hindered and a higher productivity is obtained. This finding is further confirmed by a batch experiment, in which 0.5 M (-)-isopulegol was added to the reaction mixture (Table S2 entries 10, 11, 22, 23), which leads to a significantly stronger decrease in activity for Sn-SBA-15 than Sn-Beta, due to this size-exclusion effect.

The main by-products of the studied reaction are isopulegol ethers formed through condensation reactions.[47] As such an acid-catalyzed bimolecular reaction proceeds through a bulky transition state, it is highly unlikely to occur in the small pores of the zeolite, where most of the Lewis and Brønsted acid sites are located. Sn-SBA-15 on the other hand possesses readily accessible Sn^{IV} and silanol sites and can catalyze the reverse reaction, as well as by-product formation.

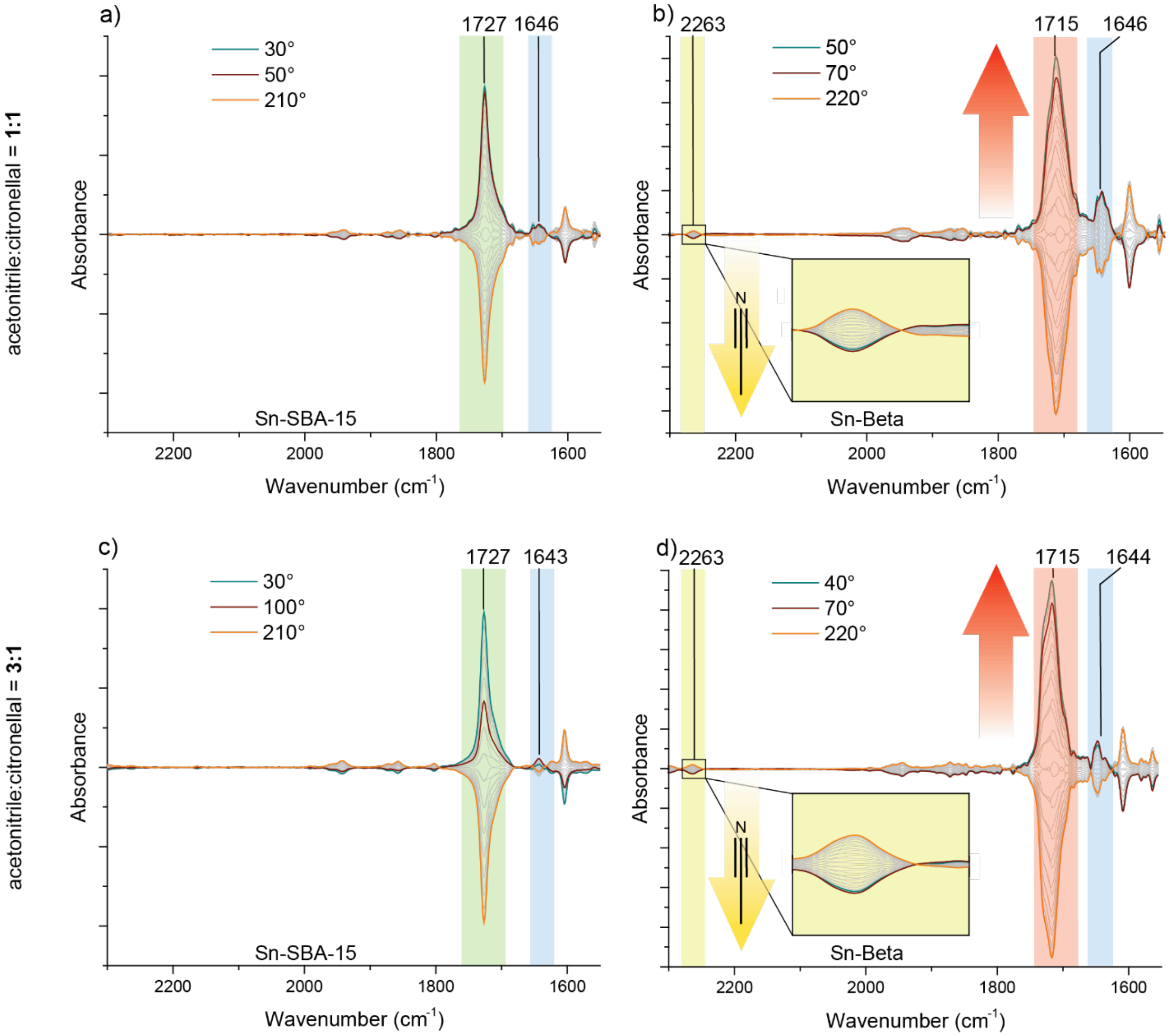

Figure 3. Phase-domain spectra for the modulation of 20 mM citronellal in a solution of 20 mM acetonitrile in toluene (top) and 60 mM acetonitrile in toluene (bottom) for Sn-SBA-15 a) and c) and Sn-Beta b) and d).

Competitive adsorption of acetonitrile and citronellal

To rationalize the vast difference in catalytic performance of Sn-SBA-15 and Sn-Beta in presence of acetonitrile (Table 1), a competitive adsorption study was performed. As the physicochemical properties of acetonitrile (higher polarity, lower refractive index than toluene) impede sensitive ATR measurements,[23,25] we decided to assess the influence of acetonitrile by adding it to toluene in different acetonitrile/citronellal ratios. In these experiments, the concentration of citronellal was modulated in presence of a constant acetonitrile concentration. As expected from batch experiments, SBA-15 is hardly active in the presence of acetonitrile. Only a liquid-phase citronellal signal appears at 1727 cm^{-1} and a small peak around 1640 cm^{-1}, assigned to minor production of isopulegol, is visible for an acetonitrile/citronellal molar ratio of 1:1. At a ratio of 3:1, the minor isopulegol signal completely disappears (Figures S33-S36). No distortion of the ν(CN) region (ca. 2263 cm^{-1}) was observed for either of the two ratios. The adsorption on Si-Beta results in similar spectra, only showing a small product peak at 1643 cm^{-1} and the liquid-phase citronellal peak. However, when the acetonitrile content was increased to a 3:1 ratio with respect to citronellal, additionally a ν(CN) vibration with negative absorbance was observed, as well as an even smaller product peak.

In the case of Sn-SBA-15 (Figure 3a), the addition of acetonitrile in a 1:1 ratio leads to the complete disappearance of the shoulder at 1712 cm^{-1} observed in pure toluene. No negative peak in the ν(CN) region can be observed which means that almost no acetonitrile is displaced from the solid-liquid interface by citronellal. A small product band at 1646 cm^{-1} reveals still minor activity. By further increasing the acetonitrile/citronellal ratio to 3:1 (Figure 3c) this band gets even smaller and still no perturbed ν(CN) peak is visible. Additionally, the small product peak shows a maximum at a phase angle of 100° showing an increased induction time until a steady product concentration is reached. Even though only a shoulder is observed in the liquid-phase CD_3CN adsorption experiment (Fig S10), indicating weak Lewis acidity, this competitive study implies that acetonitrile binds more strongly to the Sn^{IV} sites in Sn-SBA-15 than citronellal. This effect will be further amplified when pure acetonitrile is used as solvent, which results in poor activity (Table 1).

For Sn-Beta, an activated C=O peak is visible at 1715 cm^{-1} for an acetonitrile/citronellal ratio of 1:1 and 3:1 (Figures 3b and 3d). This peak is shifted by 3 cm^{-1} compared to pure toluene as solvent, indicating a minor distortion of the citronellal coordination by acetonitrile. Nevertheless, inside the zeolite pores, citronellal is able to displace acetonitrile as can be seen by the negative ν(CN) band at 2263 cm^{-1}. Furthermore, the absolute phase delay of the (liquid phase) product peak at 1646 cm^{-1} is 70°, which is 30° less than in pure toluene. A 3:1 acetonitrile/citronellal ratio also leads to a faster transport and/or adsorption of citronellal to the Sn^{IV} site, which is reflected in the 40° absolute phase delay of the peak at 1715 cm^{-1}, *i.e.* 10° less than in pure toluene.

These findings demonstrate that the addition of acetonitrile leads to facilitated transport of citronellal and isopulegol inside the zeolite pores, possibly due to the smaller molecular size of the additive and competitive adsorption/desorption. The coordination of citronellal is also stabilized in the presence of the Lewis base acetonitrile. For the mesoporous Sn-SBA-15, however, the Sn^{IV} sites are more accessible, which leads to detrimental competitive adsorption.

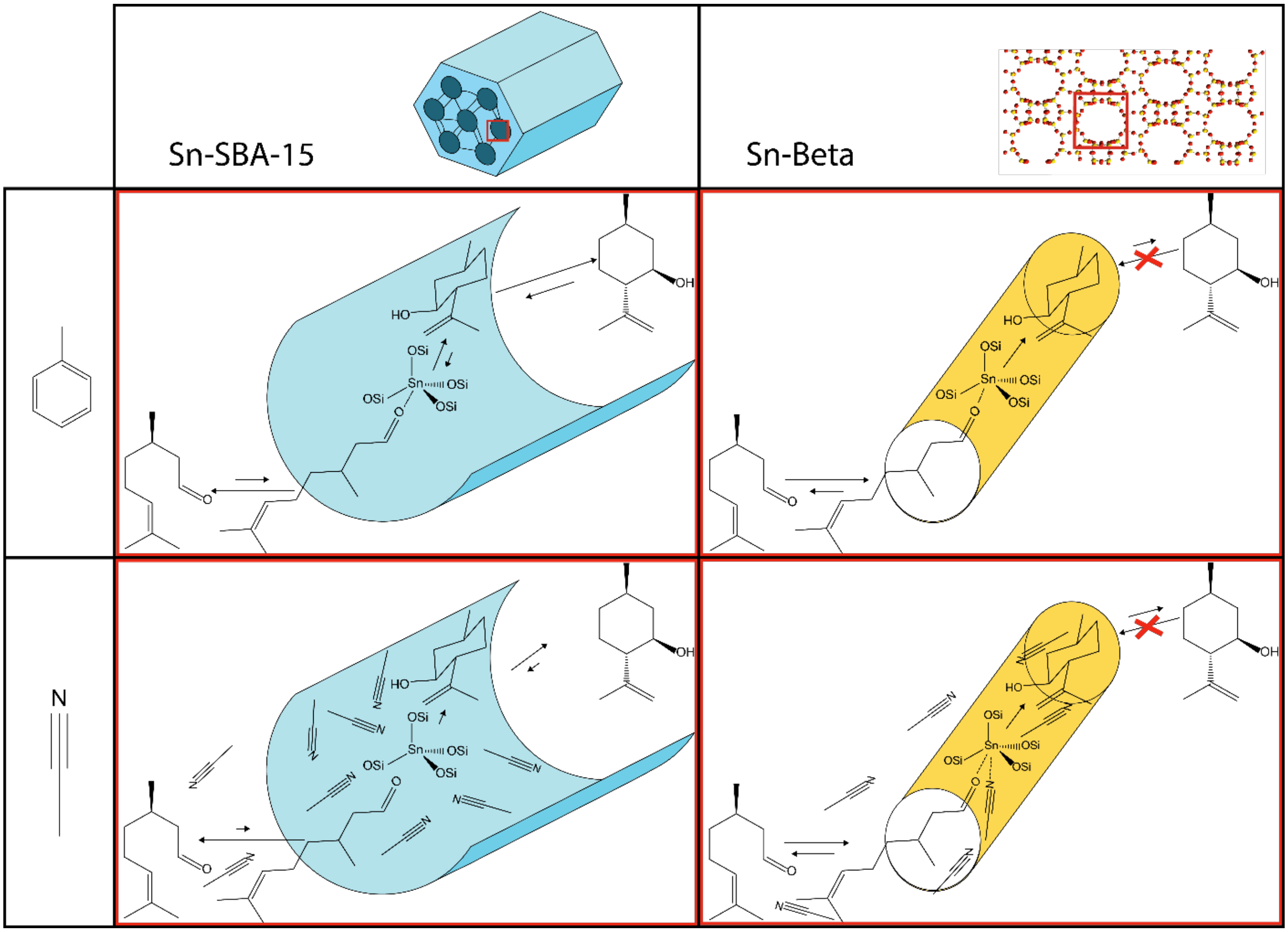

Scheme 2. Representation of effects occurring during the cyclization of citronellal over Sn-SBA-15 and Sn-Beta in the presence of acetonitrile and toluene.

DISCUSSION

On the timescale of the ATR-IR MES experiments, no significant deactivation was observed. Hence, the obtained spectroscopic data can be correlated with the reactivity of the initial phase of the batch reactions. Based on our experimental observations, the different effects influencing the cyclization of citronellal over Sn-SBA-15 and Sn-Beta are thus summarized in Scheme 2. In the case of Sn-SBA-15 in toluene, citronellal can easily diffuse to the Sn^{IV} site. The citronellal coverage on Sn^{IV} sites is relatively low, as solvent molecules can effectively interfere with the coordinated citronellal. Once the product is formed, it can easily diffuse away, but it can also re-coordinate to the site and undergo the reverse reaction, or form undesired by-products. The size-restricted micropore structure of the Beta zeolite increases the coverage of citronellal on Sn^{IV} sites. Confinement effects, as indicated by the same spectral position of the ν(C=O) vibration but a vastly different coverage for the two materials, most likely lead to a more stabilized coordination which increases the productivity. The micropore structure hinders the product from diffusing out of the pores, but also reduces by-product formation and the reverse reaction becomes unlikely as the product cannot re-enter the pore. When the Lewis base acetonitrile is used as solvent, the higher solvent concentration of the smaller molecule leads to a significant loss in activity. Our MES-ATR-IR study with 1:1 and 3:1 acetonitrile/citronellal ratios suggests a stronger interference of the solvent with citronellal coordinated to the Sn^{IV} site as a possible explanation. On the other hand, a simultaneous coordination of citronellal and acetonitrile to the Sn^{IV} site inside the micropore of Sn-Beta induces better diastereoselectivity. Similar to a bulky ligand in a homogeneous catalyst,[48,49] acetonitrile reduces the space around the active site and hence the formation of (-)-isopulegol is favored. The latter hypothesis was suggested before, but could never be observed experimentally.[21] Finally, acetonitrile leads to easier diffusion of both reactant and product in the micropores, as indicated by smaller absolute phase delays, which likely enhances the overall reactivity. The amorphous Sn-SiO_2 presents the other extreme case as the active Sn^{IV} sites are present at the external surface where the solvent can easily interfere with the coordinated citronellal. According to the liquid-phase acetonitrile adsorption (Figure S10), Sn-SiO_2 was found to be more acidic than Sn-SBA-15, but it is still less active. Hence, a plausible explanation for the difference in activity could be the much smaller total micropore volume of Sn-SiO_2 compared to Sn-SBA-15 (Table S1), *i.e.* some of the Sn^{IV} sites in Sn-SBA-15 are present in a microporous environment which might explain the higher activity. A similar effect has also been found for the conversion of tetrose sugars over Sn^{IV}-containing materials, where Sn-SBA-15 showed a different temperature-dependency than the purely mesoporous Sn-MCM-41.[2] However, this is just a hypothesis and needs further experimental validation.

As shown with the illustrative examples above, the Lewis acidity, even when measured under in situ conditions, is not a sufficient descriptor for the reactivity of stannosilicates. It is therefore highly important to gain insights into the molecular composition near the active site to understand complex heterogeneous liquid-phase catalysis. The use of MES-ATR-IR provides a unique tool to probe dynamics at the solid-liquid interface with high sensitivity.

CONCLUSIONS

In conclusion, we studied the cyclization of citronellal as a case study to get insights into solid Lewis acid catalyzed liquid-phase reactions. A combination of batch experiments and ATR-IR-MES spectroscopic investigations revealed important details on pore size and solvent effects. The reaction mechanism over Sn-SBA-15 and Sn-Beta could be followed spectroscopically and involves the coordination of citronellal with its carbonyl group to the Sn^{IV} site, followed by the cyclization step and product desorption. The coordination is amplified in Sn-Beta because of the stronger Lewis acidity and confinement effects inside the micropore. As the product isopulegol is too big to enter the pores of the Sn-Beta zeolite, by-product formation and the reverse reaction are hindered due to size exclusion resulting in a better catalytic performance. In Sn-SBA-15 on the other hand, the Sn^{IV} sites are readily accessible for substrate, product and solvent, resulting in a lower overall activity and selectivity. The addition of the Lewis base acetonitrile leads to a stronger loss in catalyst performance for Sn-SBA-15 due to competition for the Lewis acid site. This effect is not as pronounced in the microporous Sn-Beta because the local acetonitrile concentration is lower as citronellal is able to displace acetonitrile from the active site. Additionally, the simultaneous coordination of citronellal and acetonitrile enhances stereoselectivity as it beneficially reduces the space around the active site and accelerates substrate and product diffusion inside the micropores. As shown with these examples, confinement and solvent effects play an important role in understanding why certain catalytic systems are highly active. As the local molecular composition close to the active site is often not known and the reaction mechanisms are highly complex, a sensitive spectroscopic technique is crucial to obtain insights on a molecular level. ATR-IR spectroscopy in combination with MES is an ideal tool in that regard and can be applied to many other relevant heterogeneously catalyzed reactions as well.

EXPERIMENTAL DETAILS

Materials synthesis

The mesoporous SBA-15 material was synthesized according to a literature procedure:[36] 3.5 g of Pluronic P123 was fully dissolved in 62.8 g of water and 2 g of HCl (37%) at 308 K. After the addition of 7.44 g tetraethylorthosilicate (TEOS), the solution was stirred for a day. Then, the mixture was hydrothermally treated in a Teflon-lined autoclave for 42 hours at 373 K. The obtained SBA-15 was washed with 5 L of water, dried in an oven overnight at 373 K and calcined in air at 823 K for 6 h.

The mesoporous Sn-SBA-15 material was synthesized using a method reported by Selvaraj *et al.*[30,31], 4 g of Pluronic P123 was stirred with 25 mL of water to yield a clear solution. Afterwards, a dilute HCl solution was prepared by mixing 12.8 g HCl (37%) with 144.8 g of water, added to the solution, and stirred for 1 h. Then, 9 g of TEOS and 3.06 g of $SnCl_4$ were added and stirred for 24 h at 313 K. The solid products were recovered by filtration, washed several times with water and dried overnight at 373 K. Finally, the sample was calcined in air at 823 K for 6 h.

Pure Si-Beta zeolite was prepared following a literature procedure.[35] To 25.5g tetraethylammonium hydroxide solution (35 wt%, SACHEM) 23g tetraethyl orthosilicate (TEOS, 99% Sigma Aldrich) was added. The reaction mixture was stirred under ambient conditions allowing ethanol and water to evaporate until the desired final composition was obtained. After adding 2.4g of hydrofluoric acid (HF, 48 wt%, Sigma Aldrich) dropwise and homogenizing the synthesis gel with a PTFE spatula, the thick paste was transferred into a 45 mL stainless steel autoclave equipped with a PTFE liner. Hydrothermal crystallization was carried out at 140 °C and 60 rpm for 7 days. The final product was filtered, washed with water and acetone and dried at 120 °C over night. To remove the organics the sample was calcined at 853 K for 6h.

The Sn-Beta zeolite was prepared through a post-synthetic method reported elsewhere.[32-34] Dealumination of the parent commercial Al-Beta zeolite (Zeolyst, $SiO_2/Al_2O_3=300$) was done by acid leaching (13 M HNO_3, 20 mL g-1, 373 K, 20 h). Tin was incorporated via solid-solid ion-exchange by grinding dealuminated Beta with the appropriate amount of the tin(II) acetate precursor followed by subsequent heat treatments under N_2 and air for 3 h each at 823 K.

The amorphous Sn-SiO_2 material was synthesized via a xerogel method.[29] 7 g of TEOS was diluted with 8.7 g of water. 1.9 g of a 0.1 M HCl solution was added and the resulting solution was stirred for 2 hours. Then, a solution of 0.2 g of $SnCl_4 \cdot 5\ H_2O$ in 2 g of water was prepared and added dropwise to the first solution. After another hour of stirring, a 40 wt% tetrapropylammonium hydroxide solution was added dropwise until the gel hardened. The resulting gel was dried at 373 K overnight and calcined in air at 853 K for 6 h.

Ex Situ Characterization

The different materials were analyzed with various techniques: Si, Al and Sn contents were determined by ICP-OES after digesting the solids in HF. The small-angle powder XRD-patterns for calcined samples were recorded under ambient conditions on a Bruker D8 advance diffractometer with Cu Kα radiation (λ=1.5406 Å). N_2-physisorption measurements were performed on a Micromeritics 3flex apparatus. The samples were degassed prior to measurement for 4 hours at 373 K. Adsorption isotherms were collected at 77 K and analyzed using BET, t-plot and DFT methods. DRUV-Vis analysis was performed with a Maya2000 Pro spectrometer (Ocean Optics) equipped with a deuterium/halogen light source (DH-200-BAL from Mikropack) using $BaSO_4$ as matrix.

Batch reactivity

Batch reactions were performed in 10 mL thick-walled glass reactors sealed with PTFE caps under vigorous stirring at 600 rpm and were heated in a temperature controlled oil bath. Typically, the reactions were performed at 333 K with 50 mg of catalyst, and 5 ml of a 0.5 M citronellal solution for 4 hours. Biphenyl was used as an internal standard. Samples were taken periodically and analyzed using an HP6890 gas chromatograph (Agilent) equipped with an HP-5 column. By-products were mainly condensation products.

ATR-IR & MES

The preparation of a catalyst layer was done by adding 10 mL of a 1:25 times diluted Collodion solution (5%, in 75:25 diethyl ether:ethanol, Fisher Scientific) to 100 mg of catalyst. The resulting suspension was stirred for 1 hour and then sonicated for 5 minutes. 1 mL of this solution was deposited onto the ZnSe crystal and put in an oven to dry at 353 K for 30 minutes to yield ca. 9 mg of deposited catalyst. The influence of the added Collodion on reactivity was tested in a batch reaction and was only minor (see Table S2). All ATR-IR measurements were performed on a Bruker Vertex 70 spectrometer equipped with a liquid nitrogen cooled MCT detector. Typically 32 scans with a resolution of 4 cm^{-1} were co-added to give one spectrum. The switching between the two liquid reservoirs was accomplished through air-actuated valves (Parker) and modulation frequencies of 10-50 mHz. The ATR accessory was homemade and made use of a 45° ZnSe crystal. Measurements with a bare crystal showed a total exchange of the cell volume within less than 2 seconds under typical conditions. The liquids were drawn by a peristaltic pump (Ismatec) at flow rates of 3-25 ml/min. See Figure S45 for a schematic of the setup. Absorbance is given in arbitrary units for all spectra in the time- and phase-domain.

ASSOCIATED CONTENT

Supporting Information. Additional batch reactivity data, IR spectra, estimation of rate of diffusion, schematic of setup and explanation of MES experiment.

AUTHOR INFORMATION

Corresponding Author

*E-mail: hermans@chem.wisc.edu

ACKNOWLEDGEMENTS

The authors thank Sam Burt for help with XRD and Connor Firth for assistance with ICP-OES measurements. Financial support from the University of Wisconsin – Madison, the Wisconsin Alumni Research Foundation (WARF), the US Army Research Office under grant W911NF-15-1-0134 and the Swiss National Science Foundation (grant 200021_146661) is kindly acknowledged.

ABBREVIATIONS

ATR-IR, Attenuated Total Reflection Infrared; FT-IR, Fourier Transform Infrared; MES, Modulation Excitation Spectroscopy; PD, Phase-Domain; PSD, Phase Sensitive Detection; TD, Time-Domain.

REFERENCES

(1) Weisz, P. B.; Frilette, V. J.; Maatman, R. W.; Mower, E. B. *J. Catal.* **1962**, *1*, 307-312.
(2) De Clercq, R.; Dusselier, M.; Christiaens, C.; Dijkmans, J.; Iacobescu, R. I.; Pontikes, Y.; Sels, B. F. *ACS Catal.* **2015**, *5*, 5803-5811.
(3) Conrad, S.; Verel, R.; Hammond, C.; Wolf, P.; Göltl, F.; Hermans, I. *ChemCatChem* **2015**, *7*, 3270-3278.
(4) Zhou, C. H.; Xia, X.; Lin, C. X.; Tong, D. S.; Beltramini, J. *Chem. Soc. Rev.* **2011**, *40*, 5588-5617.
(5) Corma, A.; Domine, M. E.; Valencia, S. *J. Catal.* **2003**, *215*, 294-304.
(6) Qi, G. S.; Yang, R. T.; Chang, R. *Appl. Catal. B-Environ.* **2004**, *51*, 93-106.
(7) Corma, A.; Garcia, H. *Chem. Rev.* **2003**, *103*, 4307-4365.
(8) Holm, M. S.; Saravanamurugan, S.; Taarning, E. *Science* **2010**, *328*, 602-605.
(9) Dapsens, P. Y.; Mondelli, C.; Perez-Ramirez, J. *Chem. Soc. Rev.* **2015**, *44*, 7025-7043.
(10) Román-Leshkov, Y.; Moliner, M.; Labinger, J. A.; Davis, M. E. *Angew. Chem., Int. Ed.* **2010**, *49*, 8954-8957.
(11) Gunther, W. R.; Michaelis, V. K.; Caporini, M. A.; Griffin, R. G.; Román-Leshkov, Y. *J. Am. Chem. Soc.* **2014**, *136*, 6219-6222.

(12) Wolf, P.; Valla, M.; Rossini, A. J.; Comas-Vives, A.; Núñez-Zarur, F.; Malaman, B.; Lesage, A.; Emsley, L.; Copéret, C.; Hermans, I. *Angew. Chem., Int. Ed.* **2014**, *126*, 10343-10347.

(13) Van de Vyver, S.; Román-Leshkov, Y. *Angew. Chem., Int. Ed.* **2015**, *54*, 12554-12561.

(14) Boronat, M.; Concepción, P.; Corma, A.; Renz, M.; Valencia, S. *J. Catal.* **2005**, *234*, 111-118.

(15) Boronat, M.; Concepcion, P.; Corma, A.; Navarro, M. T.; Renz, M.; Valencia, S. *Phys. Chem. Chem. Phys.* **2009**, *11*, 2876-2884.

(16) Lew, C. M.; Rajabbeigi, N.; Tsapatsis, M. *Microporous Mesoporous Mater.* **2012**, *153*, 55-58.

(17) Osmundsen, C. M.; Holm, M. S.; Dahl, S.; Taarning, E. *Proc. R. Soc. A* **2012**, *468*, 2000-2016.

(18) Chung, Y.-M.; Rhee, H.-K. *J. Mol. Catal. A: Chem.* **2000**, *159*, 389-396.

(19) Wettstein, S. G.; Alonso, D. M.; Chong, Y.; Dumesic, J. A. *Energy Environ. Sci.* **2012**, *5*, 8199-8203.

(20) Farnesi Camellone, M.; Marx, D. *J. Phys. Chem. Lett.* **2013**, *4*, 514-518.

(21) Boronat, M.; Corma, A.; Renz, M. In Turning Points in Solid-State, Materials and Surface Science: A Book in Celebration of the Life and Work of Sir John Meurig Thomas; The Royal Society of Chemistry: 2008, p 639-650.

(22) Eccles, R. J. Pharm. Pharmacol. **1994**, *46*, 618-630.

(23) Mojet, B. L.; Ebbesen, S. D.; Lefferts, L. *Chem. Soc. Rev.* **2010**, *39*, 4643-4655.

(24) Zaera, F. *Chem. Soc. Rev.* **2014**, *43*, 7624-7663.

(25) Andanson, J.-M.; Baiker, A. *Chem. Soc. Rev.* **2010**, *39*, 4571-4584.

(26) Urakawa, A.; Bürgi, T.; Baiker, A. *Chem. Eng. Sci.* **2008**, *63*, 4902-4909.

(27) Meemken, F.; Maeda, N.; Hungerbühler, K.; Baiker, A. *Angew. Chem., Int. Ed.* **2012**, *51*, 8212-8216.

(28) Meemken, F.; Baiker, A.; Schenker, S.; Hungerbühler, K. *Chem. – Europ. J.* **2014**, *20*, 1298-1309.

(29) Pacheco, J. J.; Davis, M. E. *Proc. Natl. Acad. Sci. U. S. A.* **2014**, *111*, 8363-8367.

(30) Selvaraj, M.; Kawi, S. *J. Mater. Chem.* **2007**, *17*, 3610-3621.

(31) Selvaraj, M.; Choe, Y. *Appl. Catal., A* **2010**, *373*, 186-191.

(32) Hammond, C.; Conrad, S.; Hermans, I. *Angew. Chem., Int. Ed.* **2012**, *51*, 11736-11739.

(33) Wolf, P.; Hammond, C.; Conrad, S.; Hermans, I. *Dalton Trans.* **2014**, *43*, 4514-4519.

(34) Parvulescu, A. N.; Müller, U.; Teles, J. H.; Vautravers, N.; Uhl, G.; Hermans, I.; Wolf, P.; Hammond, C.; A tin-containing zeolitic material having a bea framework structure, WO2015067654 A1: 2015.

(35) Camblor, M. A.; Corma, A.; Valencia, S. *Chem. Commun.* **1996**, 2365-2366.

(36) Choi, M.; Heo, W.; Kleitz, F.; Ryoo, R. *Chem. Commun.* **2003**, 1340-1341.

(37) Corma, A.; Renz, M. *Chem. Commun.* **2004**, 550-551.

(38) Dijkmans, J.; Dusselier, M.; Janssens, W.; Trekels, M.; Vantomme, A.; Breynaert, E.; Kirschhock, C.; Sels, B. F. *ACS Catal.* **2016**, *6*, 31-46

(39) Clarke, M. L.; France, M. B. *Tetrahedron* **2008**, *64*, 9003-9031.

(40) Urakawa, A.; Bürgi, T.; Baiker, A. *Chem. Phys.* **2006**, *324*, 653-658.

(41) Baurecht, D.; Fringeli, U. P. *Rev. Sci. Instrum.* **2001**, *72*, 3782-3792.

(42) Clayden, J.; Greeves, N.; Warren, S. *Organic Chemistry*; OUP Oxford, 2012.

(43) Baerlocher, C., McCusker L.B. Database of Zeolite Structures. http://www.iza-structure.org/databases/, (accessed Oct 10, 2015).

(44) Gounder, R.; Iglesia, E. *Chem. Commun.* **2013**, *49*, 3491-3509.

(45) Allerhand, A.; von R. Schleyer, P. *J. Amer. Chem. Soc.* **1963**, *85*, 371-380.

(46) Urakawa, A.; Wirz, R.; Bürgi, T.; Baiker, A. *J. Phys. Chem. B* **2003**, *107*, 13061-13068.

(47) Fuentes, M.; Magraner, J.; De Las Pozas, C.; Roque-Malherbe, R.; Pariente, J. P.; Corma, A. *Appl. Catal.* **1989**, *47*, 367-374.

(48) Hori, Y.; Iwata, T.; Okeda, Y.; Process for producing isopulegol, US20020133046 A1: 2002.

(49) Liu, L.; Leutzsch, M.; Zheng, Y.; Alachraf, M. W.; Thiel, W.; List, B. *J. Amer. Chem. Soc.* **2015**, *137*, 13268-13271.

Graphic for Table Of Contents